Robotica: (2021) volume 39, pp. 1451–1467. © The Author(s), 2021. Published by Cambridge University Press.
doi:10.1017/S0263574720001277

Control of Teleoperation Systems in the Presence of Varying Transmission Delay, Non-passive Interaction Forces, and Model Uncertainty

Robab Ebrahimi Bavili, Ahmad Akbari and Reza Mahboobi Esfanjani*

Department of Electrical Engineering, Sahand University of Technology, Tabriz, Iran
E-mails: r.ebrahimi94@sut.ac.ir, a.akbari@sut.ac.ir

(Accepted December 4, 2020. First published online: January 8, 2021)

SUMMARY
This paper addresses robust stability and position tracking problems in teleoperation systems subject to varying delay in the communication medium, uncertainties in the models of manipulators, and non-passive interaction forces in the terminations. Fixed-structure nonlinear control law is developed based on the notion of Interconnection and Damping Assignment Passivity-Based Control (IDA-PBC) scheme. Then, utilizing the Lyapunov–Krasovskii theorem, sufficient conditions are derived in terms of Linear Matrix Inequalities (LMIs) to tune the controller parameters. Differently from literature, the objectives are achieved without requirement for any passive parts in the model of interaction forces. Comparative simulations and experimental results demonstrate the applicability and superiority of the proposed method.

KEYWORDS: Bilateral teleoperation system; Model uncertainty; Non-passive operator and environment; Asymptotic stability; Passivity-based controller.

1. Introduction

Bilateral teleoperator is a human–robot system that provides a platform for the operator to physically interact with an object in the remote environment. This system is composed of local and remote manipulators, which are connected via a communication medium. The remote robot follows the motion of local one, which is commanded by the human operator, and feeds back interaction forces from the environment to the local robot to provide a sense of telepresence.[1,2] The existence of communication delays, which degrades the system performance is one of the most significant issues in the control of bilateral teleoperation systems. The stability, position, and force tracking problems in the presence of time delay have been investigated in the studies by Nuno et al.[3] and Arcara et al.[4]

Since the physical parameters of robotic systems are difficult to be determined precisely in practice, often there are some uncertainties in their dynamical models; so, compensating the effects of these uncertainties in developing control algorithms is necessary in the design of teleoperation systems.[5] There are many adaptive schemes for compensation of the effects of uncertainties in teleoperation systems;[5–8] wherein, by online identification of the models' parameters, the destructive influences of imperfections are reduced with imposing heavy computational load.

In the framework of robust control, using μ-synthesis and H_∞ notions, controllers were developed for linear teleoperation system in the studies by Leung et al.,[9] Colgate et al.,[10] and Sirouspour.[11] A guaranteed cost control for linear bilateral teleoperation systems was developed by

* Corresponding author. E-mail: mahboobi@sut.ac.ir

Mohammadi et al.,[12] in which Linear Matrix Inequalities (LMIs) were used to ensure robust stability and performance in the presence of model uncertainty and varying transmission delay. For nonlinear teleoperation systems, only a few works in the literature consider robust stability issue. In the study by Shahdi et al.,[13] first, the local Lyapunov-based adaptive nonlinear controllers were applied to linearize the system equations and eliminate its dependency on the master and slave parameters; then, H_∞ controller was synthesized assuming constant communication delay. In the paper by Sharifi et al.,[14] a robust output feedback control strategy was presented for a nonlinear teleoperation system, which can deal with stability as well as transparency, despite the variable time delay and uncertain dynamics. First, local Lyapunov-based adaptive controllers were applied to both of master and slave sides in order to suppress the nonlinearities in the system dynamics. Then, using the Lyapunov technique, stability and performance objectives were cast as an LMI feasibility problem. Also, in the articles by Sun et al.[15] and Dinh et al.,[16] the fuzzy and neural network-based schemes were presented to address the robust stability challenge in teleoperation systems. In the most of the aforementioned works, the control law does not have a fixed structure and includes adaptive terms; so, it cannot be implemented simply in real-world systems.

On the other hand, in many applications of teleoperation systems such as mining, drilling, and beating heart surgery, the interaction forces between local robot and human operator and between remote robot and environment are not energetically passive.[17] In general, the non-passive behavior of the human or environment, which can be modeled by a constant force can deteriorate the performance of the teleoperation system or even destabilize it. Only a few papers consider this problem in the controller design for teleoperation systems. These papers can be classified into two groups. In the first cluster such as the study by Hashemzadeh et al.[18] and Ganjefar et al.,[19] there is no constraint on passivity of terminal forces; but, costly and noisy force sensors are needed for implementation of control scheme. In the second collection, without using additional force sensors, the controller is tuned to retain the stability of system despite non-passive termination.[20–23] In the work by Hua et al.,[20] a teleoperation system interacting with constant human force and passive environment was developed in the presence of varying communication delay; by using Layaounov–Krasovskii (LK) theorem, the asymptotic stability of the closed-loop system was attained by employing the Proportional Derivative controller with damping injection (PD+d). In the study by Jazayeri et al.,[21] the Llewellyn's criterion was extended to stabilize a linear teleoperator, which is in contact with non-passive human operator and environment neglecting the communication delay. The Input-to-State Stability (ISS) of non-passive teleoperator controlled by P+d control law including dynamic model terms was considered in the paper by Islam et al.,[22,23] in the presence of varying time delay; using LK theorem, criteria for boundedness of positions errors and velocity were extracted to determine the controller gains.

In the most of aforementioned papers, to obtain the Input-to–State Stability (ISS), the non-passive human operator and environment forces should satisfy hard-to-hold conditions, which relate their values to the positions and velocities of local and remote manipulators. Moreover, the stability of system relies on the existence of known passive terms in the models of interaction forces. Specifically, asymptotical stability in the paper by Hua et al.[20]or the ISS in the works by Islam et al.[22,23]was not guaranteed for arbitrary external forces. Also, the challenge of asymptotic stability of the position errors between local and remote manipulators was not considered for teleoperation systems, which are in contact with non-passive termination forces.

In this paper, we address the problem of asymptotic stability and position tracking for bilateral teleoperation systems interacting with non-passive human operator and environment, in the presence of parametric uncertainties in the models of manipulators. By extension of the notion of Interconnection and Damping Assignment Passivity-Based Control (IDA-PBC)[24]scheme to time-delay systems, a nonlinear control law that includes feedback of position errors and integral of position errors is designed for the nominal system. Then, an appropriate LK functional is employed to derive computationally amenable LMI conditions to tune the parameters of the fixed-structure IDA-PBC such that the asymptotic stability of velocities and positions errors is achieved in spite of models' uncertainties and asymmetrical varying communication delays. The main novelties of the paper are that the IDA-PBC design method is employed in the context of time-delay systems and an LK functional composed of Hamiltonian function of teleoperator system is used to derive simple conditions for robust tracking in the presence of model imperfections.

The features of the suggested scheme are summarized as follows: first, the robust asymptotic stability and position tracking in the nonlinear teleoperation system are guaranteed by a new fixed-structure controller. Second, unlike the existing methods in the literature, the developed controller leads to asymptotic stability in the system without any need for known passive parts in the dynamical model of non-passive interaction forces. Third, the asymptotic stability of the position errors in the system is provided because of using the feedback of their integrals. Fourth, no force sensors are required for practical implementation of control strategy. The results of comparative simulations and experimental verifications are presented to demonstrate the applicability and efficiency of the proposed strategy.

The rest of paper is organized as follows: Section 2 presents problem formulation and preliminaries. In Section 3, the main results in controller design and stability analysis are presented. The simulation and experimental results and comparisons are shown in Section 4. Finally, conclusions and future research directions have been discussed in Section 5.

Notation: we denote the set of real numbers by $R = (-\infty . +\infty)$, the set of all nonnegative real numbers by $R = 0$. Also, $\mathbb{R}^n$ and $\mathbb{R}^{n\times m}$ show n-dimensional real vector space and $n \times m$-dimensional real matrix space, respectively. $g^{\perp}$ symbolizes the full-rank left annihilator matrix of g, that is $g^{\perp} g = 0$. And $\nabla_x H$ stand for $\frac{\partial H}{\partial x}$. The notations $\underline{0}$ and $\underline{I} \in \mathbb{R}^{n\times m}$ denote the zero and identity matrix, respectively.

2. Problem Formulation

In this section, dynamical models of bilateral teleoperator and human operator and environment are presented. Then the problem of interest is described in detail.

2.1. Dynamical model of teleoperation system

The Euler–Lagrange equations of the considered teleoperation system comprising n-Degrees of Freedom (DOF) manipulators are as follows:[20,22,25]

$$M_l(q_l)\ddot{q}_l + C_l(q_l.\dot{q}_l)\dot{q}_l + g_l(q_l) = \tau_l{}^* + \tau_h, \tag{1}$$

$$M_r(q_r)\ddot{q}_r + C_r(q_r.\dot{q}_r)\dot{q}_r + g_r(q_r) = \tau_r{}^* - \tau_e, \tag{2}$$

where $q_i.\dot{q}_i.\ \ddot{q}_i \in \mathbb{R}^n$ for $i = l.r$ are the joint positions, velocities, and accelerations $.M_i(q_i) \in \mathbb{R}^{n\times n}$ for $i = l.r$ is the inert matrix, $C_i(q_i.\dot{q}_i) \in \mathbb{R}^{n\times n}$ is the Coriolis and centrifugal effects matrix, and $g_i(q_i) \in \mathbb{R}^n$ is the gravitational forces vector. $\tau_h \in \mathbb{R}^n$ and $\tau_e \in \mathbb{R}^n$ represent the external forces applied by the human operator and environment to the local and remote manipulators, respectively; $\tau_i{}^* \in \mathbb{R}^n$ are the control forces. Here, $i = l$ indicates the local manipulator and $i = r$ the remote one.

Model uncertainty refers to any discrepancy between a model describing a system and its true behavior. Since the physical parameters of the manipulators are difficult to obtain precisely in practice, often there are some uncertainties in Eqs. (1) and (2). These dynamical uncertainties can be modeled as additive terms to the nominal model of the system as

$$M_i(q_i) = \overline{M}_i(q_i) + \triangle M_i(q_i), \tag{3}$$

$$C_i(q_i.\dot{q}_i) = \overline{C}_i(q_i.\dot{q}_i) + \triangle C_i(q_i.\dot{q}_i), \tag{4}$$

$$g_i(q_i) = \overline{g}_i(q_i) + \triangle g_i(q_i), \tag{5}$$

where $\overline{M}_i(q_i).\overline{C}_i(q_i.\dot{q}_i)$ and $\overline{g}_i(q_i)$ are the nominal model matrices/vectors and $\triangle M_i(q_i).$ $\triangle C_i(q_i.\dot{q}_i)$and $\triangle g_i(q_i)$ are norm-bounded dynamical uncertainty matrices/vectors.

The dynamical models of manipulators presented in Eqs. (1) and (2) have the following well-known properties:[3]

Property 1. The inertia matrix $M_i(q_i)$ of a robot is symmetrical, bounded, and positive definite, that is there exists positive constant λ_m and λ_M such that $0 < \lambda_m \underline{I} \le M_i(q_i) \le \lambda_M \underline{I} < \infty$. Consequently, $0 < \rho_m \underline{I} \le M_i{}^{-1}(q_i) \le \rho_M \underline{I} < \infty$, where $\rho_m.\rho_M > 0$.

Property 2. The Coriolis and inertia matrices are related as $\dot{M}_i(q_i) = C_i(q_i.\dot{q}_i) + C_i{}^T(q_i.\dot{q}_i)$.

The control scheme presented in this paper relies on the following assumptions:

Assumption 1. *The joints' positions and velocities $(q_i.\dot{q}_i)$ are known from measurement or estimation. Note that in the absence of velocity sensors, they can be estimated using the velocity observers; for instance, by the one presented in the study by Erlic et al.*[26]

https://doi.org/10.1017/S0263574720001277 Published online by Cambridge University Press

Assumption 2. *To simplify the computations, it is assumed that the gravitational forces are locally pre-compensated; so, the dynamical model* (1) *and* (2) *are changed to*

$$M_l(q_l)\ddot{q}_l + C_l(q_l.\dot{q}_l)\dot{q}_l = \tau_l + \tau_{h,} \tag{6}$$

$$M_r(q_r)\ddot{q}_r + C_r(q_r.\dot{q}_r)\dot{q}_r = \tau_r - \tau_e. \tag{7}$$

Assumption 3. *The uncertainty matrices/vectors are norm bounded and are as follows:*

$$\|\triangle M_i(q_i)\| \le \delta_{M_i}; \qquad \|\triangle C_i(q_i.\dot{q}_i)\| \le \delta_{C_i}; \qquad \|\triangle g_i(q_i)\| \le \delta_{g_i.} \tag{8}$$

Assumption 4. *The local and remote robots exchange data by a communication channel which imposes variable time delays, $T_i(t)$ that has known upper bound.h_i, and does not grow or decrease faster than known value, μ_i, for $i = l.r$:*

$$0 < T_i(t) \le h_i < \infty, \tag{9}$$

$$\left|\dot{T}_i\right| < \mu_{i.} \tag{10}$$

2.2. Models of operator and environment

The human operator and the environment define passive velocity to force map, if there exist $\kappa_i \in R \ge 0$, such that

$$E_h(t) := -\int_0^t \dot{q}_l^T \tau_h d\sigma + \kappa_l \ \ge 0, \tag{11}$$

$$E_e(t) := \int_0^t \dot{q}_r^T \tau_e d\sigma + \kappa_r \ge 0. \tag{12}$$

Note that the signs are consistent with the standard power flow convention.[3]

The common model of non-passive human operator and environment in literature is represented utilizing a passive spring–damper system along with constant force as follows:[19,20,22]

$$\tau_h = \tau_{h_0} - S_l q_l - D_l \dot{q}_{l,} \tag{13}$$

$$\tau_e = \tau_{e_0} + S_r q_r + D_r \dot{q}_r, \tag{14}$$

where S_i and $D_i \in \mathbb{R}^{n\times n}$ denote the diagonal and positive definite matrices of the spring and damping constants and $\tau_{h_0} . \tau_{e_0} \in \mathbb{R}^n$ are constant forces. It is evident that for nonzero τ_{h_0} and τ_{e_0}, the input–output pair ($\dot{q}_l$, τ_h) and ($\dot{q}_r$,τ_e) may not satisfy (11) and (12), and hence the human operator and environment are not energetically passive. This paper aims to develop a controller to attain the asymptotic stability of system (6) and (7) interacting with unknown constant interaction forces expressed in Assumption 5.

Assumption 5. *The model of human operator and environment forces is considered by unknown constant forces $\tau_h = \tau_{h_0} . \tau_e = \tau_{e_0}$ without any known passive part in their dynamic, that is* S_i and $D_i = 0$.

It is worth noting that the passive parts of models in (13) and (14), that is, $S_i q_i$ and $D_i \dot{q}_i$ help to preserve the stability of system; however, they don't exist or aren't known in real-world applications. So, the model described in Assumption 5 is more comprehensive than the ones in literature.

The problem of interest is to determine the control forces for both of local and remote manipulators to achieve robust stable position tracking in spite of model uncertainty in the manipulators, varying time delay in data exchange between them and unknown constant interaction forces in their terminations. The schematic of the control system is depicted in Fig. 1. The IDA-PBC controllers compute the control action employing nonlinear laws, which use the measurements of positions and velocities of local and remote manipulators.

3. Main Results

In this section, first, the structure of controller is developed based on the nominal model of system for free motion ($\tau_h = \tau_e = 0$); then, the results are extended to real system with constant interaction

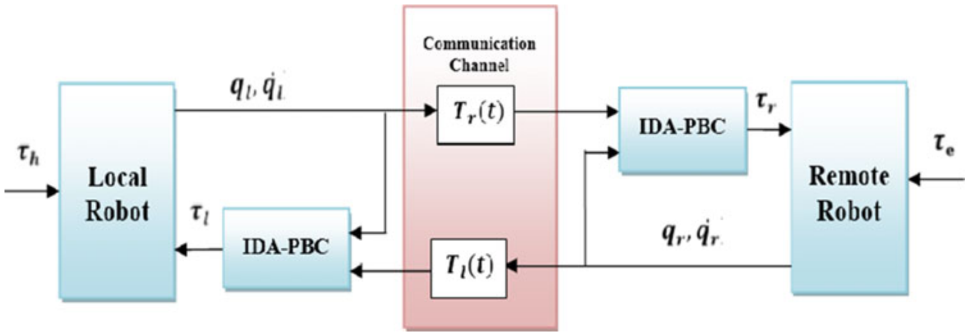

Fig. 1. Schematics of the teleoperator with the proposed control strategy.

forces (i.e., $\tau_h = \tau_{h_0}$, $\tau_e = \tau_{e_0}$). By applying LK theorem, synthesis conditions in the form of LMIs are derived for tuning the controller parameters to achieve robust stability and position tracking in the overall system.

3.1. *Design of IDA-PBC for nominal system*

To formulate the position tracking and stability objectives, we define the augmented state of system as $x_i = \left[{q_i}^T . {p_i}^T . {e_i}^T \ . \ \int_0^t e_i(s)^T ds \right]^T \in \mathbb{R}^{4n}$ for $i = l.r$, where $e_l := q_l - q_r(t - T_r(t))$ and $e_r := q_r - q_l(t - T_l(t))$ are the position errors between local and remote manipulators, and the momentum vectors of joints, p_i, are

$$p_i = \overline{M}_i(q_i)\dot{q}_{.i} \tag{15}$$

Regarding Eqs. (6) and (7) and Property 2, the affine model of nominal system is expressed as follows:

$$\dot{x}_l = f_l(x_l.x_r(t - T_r)) + g_{ul} \times (\tau_l + \tau_h), \tag{16}$$

$$\dot{x}_r = f_r(x_r.x_l(t - T_l)) + g_{ur} \times (\tau_r - \tau_e), \tag{17}$$

where for $\underline{0} \ . \underline{I} \ \in \mathbb{R}^{n \times n}$

$$f_l(x_l.x_r\ (t - T_r)) = \begin{bmatrix} \overline{M}_l^{-1}(q_l)p_l \\ \overline{C}_l^{\,T}(q_l.\dot{q}_l)\overline{M}_l^{-1}(q_l)p_l \\ \overline{M}_l^{-1}(q_l)p_l - \overline{M}_r^{-1}(q_r(t - T_r))p_r(t - T_r) \\ e_l \end{bmatrix}, \ g_{ul} = \begin{bmatrix} \underline{0} \\ \underline{I} \\ \underline{0} \\ \underline{0} \end{bmatrix}.$$

$$f_r(x_r.x_l\ (t - T_l)) = \begin{bmatrix} \overline{M}_r^{-1}(q_r)p_r \\ \overline{C}_r^{\,T}(q_r.\dot{q}_r)\overline{M}_r^{-1}(q_r)p_r \\ \overline{M}_r^{-1}(q_r)p_r - \overline{M}_l^{-1}(q_l(t - T_l))p_l(t - T_l) \\ e_r \end{bmatrix}. \qquad g_{ur} = \begin{bmatrix} \underline{0} \\ \underline{I} \\ \underline{0} \\ \underline{0} \end{bmatrix};$$

The proposed controller is designed based on (16) and (17) in what follows.

Consider the augmented model of local manipulator (16) with $\tau_h = 0$. The aim is to find a control torque τ_l such that the resulting closed loop of local subsystem (16) be as the following delayed Port-Hamiltonian form

$$\dot{x}_l = F_l \nabla_{x_l} H_l\ (x_l.x_r\ (t - T_r)) + \tilde{F}_r \nabla_{x_r(t-T_r)} H_l\ (x_l.x_r\ (t - T_r)), \tag{18}$$

https://doi.org/10.1017/S0263574720001277 Published online by Cambridge University Press

where F_l and $\tilde{F}_r \in \mathbb{R}^{4n\times 4n}$ are the interconnection/damping matrices of closed-loop system. Desired closed-loop Hamiltonian function is chosen to be as

$$H_l(x_l, x_r\ (t-T_r)) = \frac{1}{2}{x_l}^T x_l + \frac{1}{2}x_r(t-T_r)^T x_r(t-T_r) \tag{19}$$

which is the sum of desired kinetic energy and desired potential energy. Therefore, the Eq. (18) is rewritten as follows:

$$\dot{x}_l = F_l x_l + \tilde{F}_r x_r\ (t-T_r\}. \tag{20}$$

By considering the full-rank left annihilator of input matrix of augmented system, $g_{ul}.\ as\ \ g_{ul}^{\perp}(x_l) = \left[\underline{0}\ \underline{0}\ \underline{I}\ \underline{0}\right];\ \underline{0}\ .\ \underline{I} \in \mathbb{R}^{n\times n}$, the matching equation is

$$g_{ul}^{\perp}(x_l)\left(F_l x_l + \tilde{F}_r x_r\ (t-T_r) - f_l\ (x_l.x_r\ (t-T_r))\right) = 0 \tag{21}$$

which can be trivially solved by

$$F_l = \begin{bmatrix} \underline{0} & \overline{M_l}^{-1}(q_l) & \underline{0} & \underline{0} \\ f_{21} & f_{22} & f_{23} & f_{24} \\ \underline{0} & \overline{M_l}^{-1}(q_l) & \underline{0} & \underline{0} \\ \underline{0} & \underline{0} & \underline{I} & \underline{0} \end{bmatrix},\ \tilde{F}_r = \begin{bmatrix} \underline{0} & \underline{0} & \underline{0} & \underline{0} \\ \underline{0} & \underline{0} & \underline{0} & \underline{0} \\ \underline{0} & -\overline{M_r}^{-1}(q_r(t-T_r)) & \underline{0} & \underline{0} \\ \underline{0} & \underline{0} & \underline{0} & \underline{0} \end{bmatrix}, \tag{22}$$

where $f_{21}.\ f_{22}\ .\ f_{23}$ and $f_{24} \in \mathbb{R}^{n\times n}$ are free parameters. So, the control law is obtained as follows:

$$\tau_l = \left(g_{ul}^T g_{ul}\right)^{-1} g_{ul}^T \left(F_l x_l + \tilde{F}_r x_r\ (t-T_r) - f_l\ (x_l.x_r\ (t-T_r))\right). \tag{23}$$

Similarly, for the remote manipulator model, (17), when $\tau_e = 0$, we have

$$\tau_r = \left(g_{ur}^T g_{ur}\right)^{-1} g_{ur}^T \left(F_r x_r + \tilde{F}_l x_l\ (t-T_l) - f_r\ (x_r.x_l(t-T_l))\right) \tag{24}$$

in which

$$F_r = \begin{bmatrix} \underline{0} & \overline{M_r}^{-1}(q_r) & \underline{0} & \underline{0} \\ f_{55} & f_{56} & f_{57} & f_{58} \\ \underline{0} & \overline{M_r}^{-1}(q_r) & \underline{0} & \underline{0} \\ \underline{0} & \underline{0} & \underline{I} & \underline{0} \end{bmatrix},\ \tilde{F}_l = \begin{bmatrix} \underline{0} & \underline{0} & \underline{0} & \underline{0} \\ \underline{0} & \underline{0} & \underline{0} & \underline{0} \\ \underline{0} & -\overline{M_l}^{-1}(q_l(t-T_l)) & \underline{0} & \underline{0} \\ \underline{0} & \underline{0} & \underline{0} & \underline{0} \end{bmatrix} \tag{25}$$

with

$$H_r(x_r.x_l\ (t-T_l)) = \frac{1}{2}{x_r}^T x_r + \frac{1}{2}x_l\ (t-T_l)^T x_l\ (t-T_l). \tag{26}$$

The free parameters of F_i are determined in the next subsection such that the robust stability in position tracking is achieved for the real system.

Briefly, considering gravity pre-compensation, the final nonlinear control law is obtained from (23) and (24) by straightforward manipulation as

$$\tau_l^* = \overline{g}_l(q_l) + \tau_l = \overline{g}_l(q_l) - \overline{C_l}^T(q_l.\dot{q}_l)\dot{q}_l + f_{21}q_l + f_{22}\overline{M}_l(q_l)\dot{q}_l + f_{23}\,e_l + f_{24}\int_0^t e_l(s)ds, \tag{27}$$

$$\tau_r^* = \overline{g}_r(q_r) + \tau_r = \overline{g}_r(q_r) - \overline{C_r}^T(q_r.\dot{q}_r)\dot{q}_r + f_{55}q_r + f_{56}\overline{M}_r(q_r)\dot{q}_r + f_{57}\,e_r + f_{58}\int_0^t e_r(s)ds. \tag{28}$$

https://doi.org/10.1017/S0263574720001277 Published online by Cambridge University Press

The aforementioned strategy to obtain IDA-PBC parameters is known as algebraic IDA-PBC in which the desired energy function is fixed and the matching equation of IDA-PBC is an algebraic equation of unknown elements of F_i.

3.2. Robust stability

Now consider the teleoperation (1) and (2) with IDA-PBC control law (27) and (28) in contact with constant interaction forces $\tau_h = \tau_{h_0}$. $\tau_e = \tau_{e_0}$. Now, the closed-loop system is

$$\begin{aligned} &M_l(q_l)\ddot{q}_l + C_l(q_l.\dot{q}_l)\dot{q}_l + (\overline{g}_l(q_l) + \triangle g_l(q_l)) \\ &\quad = \overline{g}_l(q_l) - \overline{C}_l^{\,T}(q_l.\dot{q}_l)\dot{q}_l + f_{21}q_l + f_{22}\overline{M}_l(q_l)\dot{q}_l + f_{23}\,e_l + f_{24}\int_0^t e_l(s)ds + \tau_{h_0,} \qquad (29)\\ &M_r(q_r)\ddot{q}_r + C_r(q_r.\dot{q}_r)\dot{q}_r + (\overline{g}_r(q_r) + \triangle g_r(q_r)) \\ &\quad = \overline{g}_r(q_r) - \overline{C}_r^{\,T}(q_r.\dot{q}_r)\dot{q}_r + f_{55}q_r + f_{56}\overline{M}_r(q_r)\dot{q}_r + f_{57}\,e_r + f_{58}\int_0^t e_r(s)ds - \tau_{e_0}. \qquad (30)\end{aligned}$$

The momentum vectors dynamics are computed as

$$\dot{p}_i = \dot{M}_i(q_i)\dot{q}_i + M_i(q_i)\ddot{q}_i \qquad (31)$$

Regarding Eqs. (29) and (30) and Property 2, momentum vectors dynamics are

$$\dot{p}_l = \triangle C_l^{\,T}(q_l.\dot{q}_l)\dot{q}_l - \triangle g_l(q_l) + f_{21}q_l + f_{22}\overline{M}_l(q_l)\dot{q}_l + f_{23}\,e_l + f_{24}\int_0^t e_l(s)ds + \tau_{h_0,} \qquad (32)$$

$$\dot{p}_r = \triangle C_r^{\,T}(q_r.\dot{q}_r)\dot{q}_r - \triangle g_r(q_r) + f_{55}q_r + f_{56}\overline{M}_r(q_r)\dot{q}_r + f_{57}\,e_r + f_{58}\int_0^t e_r(s)ds - \tau_{e_0}. \qquad (33)$$

Define $X_l = [{q_l}^T . \int_0^t e_l(s)^T ds\ .{p_l}^T]^T \in \mathbb{R}^{3n}$ and $X_{\mathrm{r}} = [{q_r}^T\ .\ \int_0^t e_r(s)^T ds.{p_r}^T]^T \in \mathbb{R}^{3n}$, the closed-loop system is described as follows:

$$\dot{X}_l = A_x X_l + A_{xy} X_r\,(t - T_r) + g_x \times (\tau_{h_0} - \triangle g_l(q_l)), \qquad (34)$$

$$\dot{X}_r = A_y X_r + A_{yx} X_l\,(t - T_l) + g_y \times \left(-\tau_{e_0} - \triangle g_r(q_r)\right), \qquad (35)$$

where

$$A_x := \begin{bmatrix} \underline{0} & \underline{0} & {M_l}^{-1}(q_l) \\ \underline{I} & \underline{0} & \underline{0} \\ \alpha_x & f_{24} & \beta_x \end{bmatrix}. \qquad A_{xy} := \begin{bmatrix} \underline{0} & \underline{0} & \underline{0} \\ -\underline{I} & \underline{0} & \underline{0} \\ -f_{23} & \underline{0} & \underline{0} \end{bmatrix}.$$

$$g_x := \begin{bmatrix} \underline{0} \\ \underline{0} \\ \underline{I} \end{bmatrix}. \alpha_x = f_{21} + f_{23};\ \beta_x = \left(\triangle C_l^{\,T}(q_l.\dot{q}_l) + f_{22}\overline{M}_l(q_l)\right) M_l^{-1}(q_l),$$

$$A_y := \begin{bmatrix} \underline{0} & \underline{0} & {M_r}^{-1}(q_r) \\ \underline{I} & \underline{0} & \underline{0} \\ \alpha_y & f_{58} & \beta_y \end{bmatrix}. \qquad A_{yx} := \begin{bmatrix} \underline{0} & \underline{0} & \underline{0} \\ -\underline{I} & \underline{0} & \underline{0} \\ -f_{57} & \underline{0} & \underline{0} \end{bmatrix}.$$

$$g_y := \begin{bmatrix} \underline{0} \\ \underline{0} \\ \underline{I} \end{bmatrix} \alpha_y = f_{55} + f_{57}.\beta_y = \left(\triangle C_r^{\,T}(q_r.\dot{q}_r) + f_{56}\overline{M}_r(q_r)\right) M_r^{-1}\,(q_r\}.$$

https://doi.org/10.1017/S0263574720001277 Published online by Cambridge University Press

From (32) and (33), the equilibrium points of positions denoted by $q_l{}^*$. $q_r{}^*$ satisfy

$$-\left(f_{21}q_l{}^* + f_{23}\, e_l{}^* + f_{24}\int_0^{t^*} e_l(s)ds\right) = \tau_{h_0} - \triangle g_l\left(q_l{}^*\right), \tag{36}$$

$$f_{55}q_r{}^* + f_{57}\, e_r{}^* + f_{58}\int_0^{t^*} e_r(s)ds = \tau_{e_0} + \triangle g_r\left(q_r{}^*\right), \tag{37}$$

where $e_l{}^* = -\, e_r{}^* = q_l{}^* -\, q_r{}^* = 0$.

Let $x = X_l - X_l{}^*$, and $y = X_r - X_r{}^*$ where $X_i{}^* = \left[q_i{}^{*T} . \int_0^{t^*} e_i(s)^T ds\ .\underline{0}\right]^T$ is the equilibrium points of X_i, where $\int_0^{t^*} e_i(s)^T = constant$. Regarding (36) and (37), Eqs. (34) and (35) are rewritten as

$$\dot{x} = A_x x + A_{xy}\ \ y\,(t - T_r), \tag{38}$$

$$\dot{y} = A_y\ y + A_{yx}\ x\,(t - T_l\}. \tag{39}$$

Remark 1. When there is no uncertainty in system, that is the nominal case, the system is expressed by (38) and (39) with $\beta_x = f_{22}$ and $\beta_y = f_{56}$.

In the following theorem by using LK argument, LMI conditions are derived to tune efficiently the free parameters of the control laws (27) and (28) such that the closed-loop system (38) and (39) be robustly asymptotically stable.

Theorem 1. *The system (38) and (39) is robustly asymptotically stable provided that the constant matrix $Q = Q^T > 0$ with appropriate dimensions exist such that*

$$\pi_x := 2A_x Q + A_{xy}\ Q\ A_{xy}{}^T + (\xi_l + h_l)Q < 0, \tag{40}$$

$$\pi_y := 2A_y Q + A_{yx}\ Q\ A_{yx}{}^T + (\xi_r + h_r)Q < 0, \tag{41}$$

where $\xi_l := \frac{1}{1-\mu_l}\ \ .\ \xi_r := \frac{1}{1-\mu_r}$.

Proof. The LK functional is selected as below:

$$V := V_1 + V_2 + V_3, \tag{42}$$

where

$$V_1 = x^T P x + y^T P y,$$
$$V_2 = \xi_l \int_{t-T_l(t)}^{t} x^T(s)Px(s)ds + \xi_r \int_{t-T_r(t)}^{t} y^T(s)Py(s)ds,$$
$$V_3 = \int_{-h_l}^{0}\int_{t+\theta}^{t} x^T(s)Px(s)dsd\theta + \int_{-h_r}^{0}\int_{t+\theta}^{t} y^T(s)Py(s)dsd\theta,$$

where $P = P^T > 0$. The time derivative of V_1 along the system (38) and (39) is

$$\dot{V}_1 = 2x^T\ P\dot{x} + 2y^T\ P\dot{y} = 2x^T\ PA_x\ x + 2x^T\ PA_{xy}y\,(t - T_r) + 2\ y^T\ PA_y\ y$$
$$+ 2y^T\ PA_{yx}x\,(t - T_l\}. \tag{43}$$

By using the inequality $2a^T b \le a^T Ma + b^T M^{-1}b$, the upper bound of cross terms is obtained as below:

$$2\ \underbrace{x^T\ PA_{xy}}_{a^T}\underbrace{y\,(t - T_r)}_{b} \le \underbrace{x^T\ PA_{xy}}_{a^T}\underbrace{P^{-1}}_{M}\underbrace{x^T\ PA_{xy}}_{a} + \underbrace{y\,(t - T_r)^T}_{b^T}\underbrace{P}_{M^{-1}}\underbrace{y\,(t - T_r)}_{b}. \tag{44}$$

Similarly,

$$2y^T\ PA_{yx}x\,(t - T_l) \le y^T\ PA_{yx}P^{-1}A_{yx}{}^T P\ y + x\,(t - T_l)^T P\ x\,(t - T_l\}. \tag{45}$$

https://doi.org/10.1017/S0263574720001277 Published online by Cambridge University Press

So, we have

$$\dot{V}_1 \leq 2x^T\ PA_x\ x + x^T\ PA_{xy}P^{-1}{A_{xy}}^T P\ x + y\,(t-T_r)^T P\ y\,(t-T_r) + 2y^T\ PA_y\ \ y$$
$$+\, y^T\ PA_{yx}P^{-1}{A_{yx}}^T P\ y + x\,(t-T_l)^T P\ x\,(t-T_l\}. \tag{46}$$

Also, the time derivative of V_2 and V_3 along the system trajectories are computed as

$$\dot{V}_2 = \xi_l x^T\ P\ x - \xi_l\left(1-\dot{T}_l\right) x\,(t-T_l)^T \mathrm{P}x\,(t-T_l) + \xi_r y^T \mathrm{P}\ y$$
$$-\,\xi_r\left(1-\dot{T}_r\right)\ y\,(t-T_r)^T\ Py\,(t-T_r\}. \tag{47}$$

Regarding delay characteristics in Assumption 4, the upper bound of $\dot{V}_2$ is

$$\dot{V}_2 \leq\ \xi_l x^T\ P\ x - \xi_l(1-\mu_l)\ \ x\,(t-T_l)^T \mathrm{P}x\,(t-T_l) + \xi_r y^T \mathrm{P}\ y$$
$$-\,\xi_r\,(1-\mu_r)\ y\,(t-T_r)^T\ \ P\ y\,(t-T_r) \tag{48}$$

and $\dot{V}_3$ is calculated as

$$\dot{V}_3 = \int_{-h_l}^{0}\{x^T\ P\ x - x^T(t+\theta)\ P\ x(t+\theta)\}d\theta + \int_{-h_r}^{0}\{y^T\ P\ y - y^T(t+\theta)\ P\ y(t+\theta)\}d\theta$$
$$= h_l x^T\ P\ x - \int_{t-h_l}^{t} x^T\ (t+\theta)\ Px\,(t+\theta)d\theta + h_r y^T \mathrm{P}\ y - \int_{t-h_r}^{t} y^T\ (t+\theta)\ Py\,(t+\theta)d\theta. \tag{49}$$

Finally, by considering Eqs. (46), (48)–(49), the upper bound of $\dot{V}$ is obtained as

$$\dot{V} \leq x^T\left(2PA_x + PA_{xy}P^{-1}{A_{xy}}^T P + (\xi_l + h_l)\ P\right)x$$
$$+\, y^T\left(2PA_y + PA_{yx}P^{-1}{A_{yx}}^T P + (\xi_r + h_r)\ P\right)y$$
$$+\, x\,(t-T_l)^T P(I - \xi_l\,(1-\mu_l))x\,(t-T_l) + y\,(t-T_r)^T\ P\,(I - \xi_r\,(1-\mu_r))\ y\,(t-T_r\}. \tag{50}$$

By multiplying $P^{-1} := Q$ to left and right side of the upper bound of $\dot{V}$, we have

$$\dot{V}\ \leq\ x^T\left(2\ A_x Q + A_{xy}\ Q\ {A_{xy}}^T + (\xi_l + h_l)\ Q\right)x + y^T\left(2A_y Q + A_{yx}\ Q\ {A_{yx}}^T + (\xi_r + h_r)\ Q\right)$$
$$y =:\ x^T\pi_x\ x + y^T\pi_y\ y. \tag{51}$$

Now, to assure asymptotic stability from LK theorem, the matrices in the two quadratic terms in (51) must be negative definite; namely, $\pi_x < 0$ and $\pi_y < 0$. By proper choosing of gains, $x = X_l - {X_l}^* \to 0$, and $y = X_r - {X_r}^* \to 0$ when $t \to \infty$. Regarding Property 1, from $p_i = M_i(q_i)\dot{q}_i \to 0$ we have $\dot{q}_i \to 0$ when $t \to \infty$. Also, $\int_0^t e_i(s)^T ds \to constant$ results that $e_i(t) \to 0\ when\ t \to \infty$.

It should be noted that from Assumption 3, the parameters β_x and β_y in π_x and π_y are bounded as $\underline{\beta}_x < \beta_x < \overline{\beta}_x$and $\underline{\beta}_y < \beta_y < \overline{\beta}_y$; so, the set of LMIs (40) and (41) should be satisfied in the corners, $\underline{\beta}_x . \overline{\beta}_x . \underline{\beta}_y$ and $\overline{\beta}_y$

Remark 2. In order to determine the gains of the control laws (27) and (28), first, boundary values of uncertainty intervals, $\underline{\beta}_x . \overline{\beta}_x . \underline{\beta}_y$ and $\overline{\beta}_y$ are replaced separately in model parameters in (38) and (39), which are later substituted in inequalities (40) and (41). This procedure leads to 16 concurrent LMIs that are solved easily by commercial software like LMI Toolbox of MATLAB®. Concisely, the free parameters in the control law, F_{i} s are obtained offline by checking the feasibility of some simple LMIs.

Remark 3. Differently from the adaptive methods[5–8] which tackle the problem of model uncertainties by computationally demanding online identification of models' parameters, a fixed-structure controller as (27)–(28) is used here to compensate for the effects of dynamical uncertainties in nonlinear teleoperation system.

Remark 4. Unlike the rival methods[20–23] in which attaining closed-loop stability relies on the restrictive assumption for the existence of known passive part in interaction forces; one advantage

https://doi.org/10.1017/S0263574720001277 Published online by Cambridge University Press

Table I. The parameters of manipulators.

Parameters	Symbol	Value
Mass of first link	m_{1_i}	0.11 ∓ 0.011 kg
Mass of second link	m_{2_i}	0.14 ∓ 0.014 kg
Length of first link	l_{1_i}	0.2 m
Length of second link	l_{2_i}	0.18 m

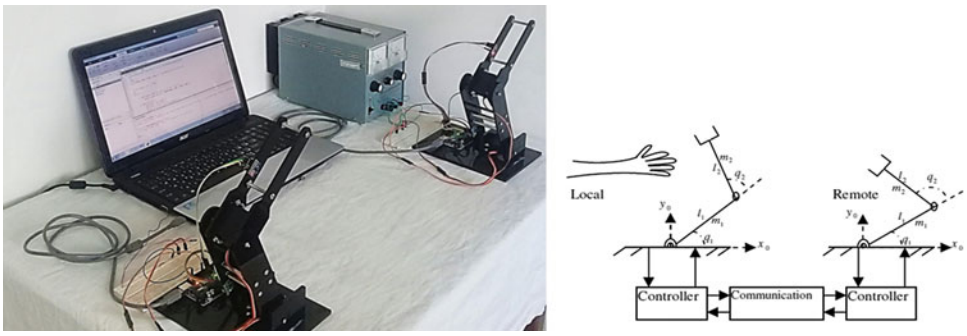

Fig. 2. Considered teleoperation system with two degrees of freedom manipulators.

of the developed controller is that by incorporating position feedback terms in the control law (i.e., $f_{21}q_l$ and $f_{55}q_r$), asymptotic stability is achieved in the presence of non-passive interaction forces without the need for passive parts (specially S_iq_i) in their dynamical models; (13)–(14). Namely, when the term S_iq_i in interaction forces exist, the non-passive part of interaction force (i.e., $\tau_{h_0} . \tau_{e_0}$) are locally damped and the system preserves its stability. Moreover, the proposed controller can provide stability of system when the interaction forces are active (i.e., $\tau_h = +S_lq_l + D_l\dot{q}_l . \tau_e = -S_rq_r - D_r\dot{q}_r$) by setting the controller parameters as $f_{21} > S_l$ and $f_{55} > S_r$. Whereas, the mentioned methods can't provide asymptotic stability in contact with active interaction forces.

Remark 5. When the interaction forces have known passive part dynamic as (13) and (14), the overall system is as (38) and (39) where $\alpha_x = f_{21} + f_{23} - S_l$, $\beta_x = (\triangle {C_l}^T(q_l.\dot{q}_l) + f_{22}\overline{M}_l(q_l) - D_l)M_l^{-1}(q_l)$, $\alpha_y = f_{55} + f_{57} - S_r$,$\beta_y = (\triangle {C_r}^T(q_r.\dot{q}_r) + f_{56}\overline{M}_r(q_r) - D_r)M_r^{-1}(q_r)$. In the presence of these known passive terms, the conservatism of stability condition is reduced.

4. Simulation and Experimental Results

In order to verify the merits and real-world applicability of the proposed control method, both simulation and experimental results are provided for the laboratory teleoperation system with 2-DOF manipulators, as shown in Fig. 2, whose parameters are listed in Table I. The knowledge about the masses of the links has 10% uncertainty.

The nonlinear model of system is expressed by Eqs. (1) and (2) and have the following inertia, Coriolis/centrifugal and gravity matrices/vector:

$$M_i(q_i) = \begin{bmatrix} M_{i_{11}} & M_{i_{12}} \\ M_{i_{21}} & M_{i_{22}} \end{bmatrix} . \ C_i(q_i.\dot{q}_i) = \begin{bmatrix} C_{i_{11}} & C_{i_{12}} \\ C_{i_{21}} & C_{i_{22}} \end{bmatrix} . \ g_i(q_i) = \begin{bmatrix} g_{i\,1} \\ g_{i\,2} \end{bmatrix},$$

where for $i \in \{l.r\}$. $M_{i_{11}} = l_{2_i}^2 m_{2_i} + l_{1_i}^2(m_{1_i} + m_{2_i}) + 2\, l_{1_i} l_{2_i} m_{2_i}\cos(q_{2_i})$, $M_{i_{12}} = M_{i_{21}} = l_{2_i}^2 m_{2_i} + l_{1_i} l_{2_i} m_{2_i}\cos(q_{2_i})$, $M_{i_{22}} = l_{2_i}^2 m_{2_i}$, $C_{i_{11}} = -2\ l_{1_i} l_{2_i} m_{2_i}\sin(q_{2_i})\dot{q}_{2_i}$, $C_{i_{12}} = -l_{1_i} l_{2_i} m_{2_i}\sin(q_{2_i})\dot{q}_{2_i}$, $C_{i_{21}} = l_{1_i} l_{2_i} m_{2_i}\sin(q_{2_i})\dot{q}_{1_i}$, $C_{i_{22}} = 0$, $g_{i\,1} = g\ \ l_{2_i} m_{2_i}\cos(q_{1_i} + q_{2_i}) + l_{1_i}(m_{1_i} + m_{2_i})\ \cos(q_{1_i})$, $g_{i\,2} = g l_{2_i} m_{2_i}\cos(q_{1_i} + q_{2_i})$. Here, $q_{k_i} . k \in \{1.2\}$ is the angular position of each link. In the simulations, the actual masses are varied randomly in the intervals confined by $\mp$10% of their nominal values to obtain the actual amounts; namely,

$$m_{1_i} \in [\underbrace{0.11}_{\overline{m}_{1_i}} - \underbrace{0.011}_{\triangle m_{1_i}} \ . \ \underbrace{0.11}_{\overline{m}_{1_i}} + \underbrace{0.011}_{\triangle m_{1_i}}; \quad m_{2_i} \in [\underbrace{0.14}_{\overline{m}_{2_i}} - \underbrace{0.014}_{\triangle m_{2_i}}, \underbrace{0.14}_{\overline{m}_{2_i}} + \underbrace{0.014}_{\triangle m_{2_i}}],$$

https://doi.org/10.1017/S0263574720001277 Published online by Cambridge University Press

Table II. System and controller parameters.

	System parameters			IDA-PBC controller parameters			
	$\delta_{M_i} \delta_{C_i} \delta_{g_i}$			$f_{21} \cdot f_{55}$	$f_{22} \cdot f_{56}$	$f_{23} \cdot f_{57}$	$f_{24} \cdot f_{58}$
Nominal system	0	0	0	$-I$	$-12I$	$-1.5I$	$-0.01I$
Uncertain system	0.0028	0.0012	0.98	$-1.3I$	$-14I$	$-1.5I$	$-0.01I$

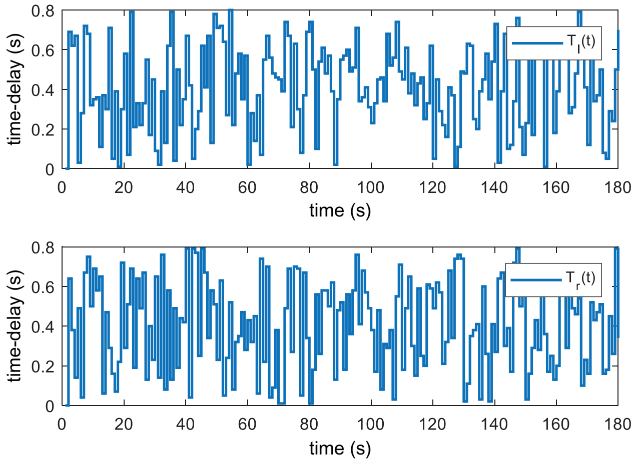

Fig. 3. The variable time delays in the forward and backward paths of communication channel.

where $\overline{m}_{1_i}$ and $\overline{m}_{2_i}$ denote the nominal amounts; $\triangle m_{1_i} = \frac{10}{100}\overline{m}_{1_i}$ and $\triangle m_{2_i} = \frac{10}{100}\overline{m}_{2_i}$ represent 10% uncertainties. It is evident that $0.0006\ I < M_i(q_i) < 0.031\ I$; $I \in \mathbb{R}^{2\times2}$. The time delays in forward and backward paths of communication channel are considered random and are shown in Fig. 3. So, the lower and upper bounds of delays and their derivative are $h_l = 0.8$, $h_r = 0.79$, $\mu_l = 0.72$, $\mu_r = 0.75$.

4.1. *Comparative simulations*

In this subsection, the teleoperation system, as shown in Fig. 2 with the designed IDA-PBC controller is simulated by MATLAB®, and the results are compared to the ones obtained by the control method proposed by Islam et al.[22]

Using the LMI toolbox of MATLAB®, the parameters of IDA-PBC controller (27) and (28) are obtained from Theorem 1 as expressed in Table II; $I \in \mathbb{R}^{2\times2}$ denotes identity matrix. The parameters of system in Table II are derived with the assumption $|\dot{q}_i| \leq\ 1.5$ rad/sec.

On the other hand, the rival controls adopted from Islam et al.[22] are as follows:

$$\tau_l^* = \overline{g}_l(q_l) + \overline{C}_l(q_l.\dot{q}_l)\dot{q}_l - k_{pl}(q_l - q_r(t - T_r(t))) - k_{dl}\dot{q}_l, \tag{52}$$

$$\tau_r^* = \overline{g}_r(q_r) + \overline{C}_r(q_r.\dot{q}_r)\dot{q}_r + k_{pl}(q_l(t - T_l(t)) - q_r) - k_{dl}\dot{q}_r, \tag{53}$$

where $k_{pl} = 1.5\ I$. $k_{dl} = 0.5I$; $I \in \mathbb{R}^{2\times2}$. The simulations are performed for two different types of interaction scenarios. For the fair comparison, the first scenario is exactly similar to the one presented in the study by Islam et al.[22] and in the second scenario, a more comprehensive case is simulated.

4.1.1. *Scenario #1.*

In the first scenario, the interaction forces between human and local manipulators and between environment and remote manipulators are considered to be non-passive as in the study by Islam et al.,[22] that is the model of (13) and (14) is considered with known passive part, whose parameters are $S_l = I$. $D_l = I$. $S_r = I$ and $D_r = I$.; $I\ \in \mathbb{R}^{2\times2}$ and τ_{h0} and τ_{e0} are bounded signals as depicted in Fig. 4.

The position tracking of teleoperation system and the velocity of manipulations in the presence of variable time delay in communication channel, uncertainties in the manipulators' models, and non-passive interaction forces in terminations are depicted in Figs. 5–6, respectively. Also control forces are shown in Fig. 7. The initial conditions are chosen to be as $q_l = \dot{q}_l = \dot{q}_r = [0\ \ 0]^T$. $q_r = [0.1\ \ 0.1]^T$.

https://doi.org/10.1017/S0263574720001277 Published online by Cambridge University Press

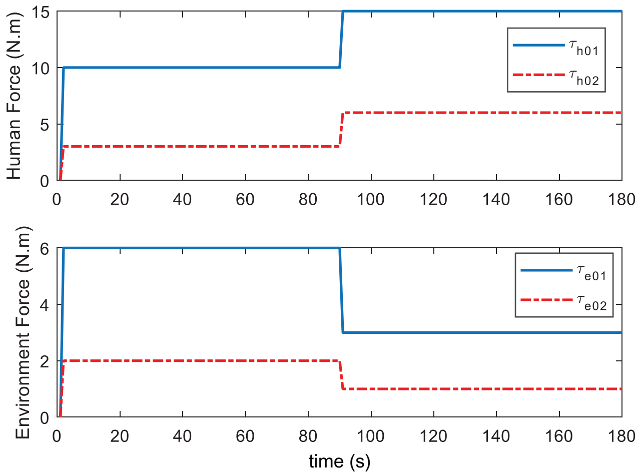

Fig. 4. The profile of the constant parts of non-passive interaction forces (τ_{h0}, τ_{e0}).

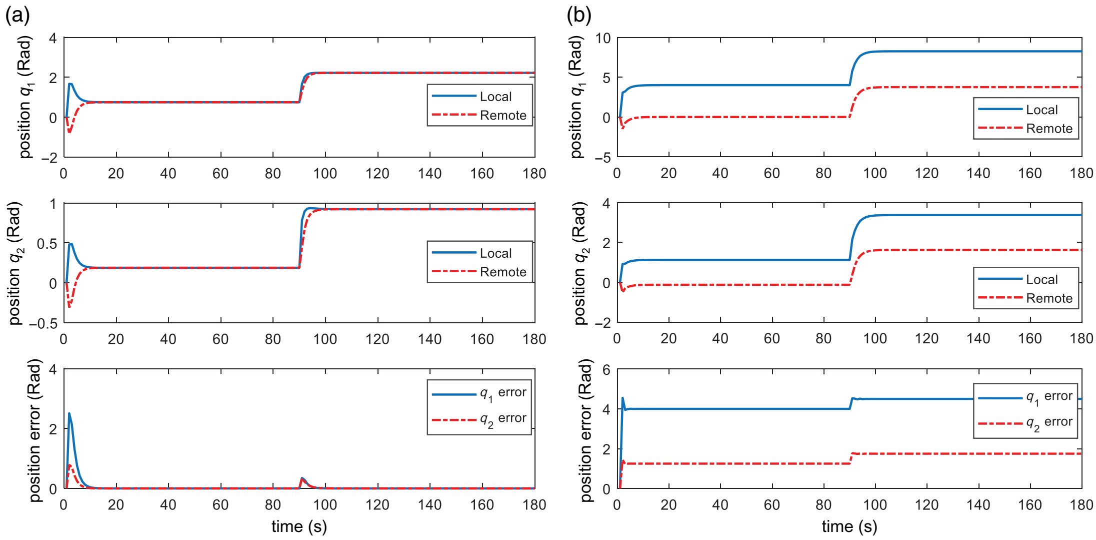

Fig. 5. Positions and positions errors in the joint space for teleoperation system in contact with non-passive interaction forces with known passive part, scenario #1, controlled by (a) proposed scheme, (b) method of Islam et al.[22]

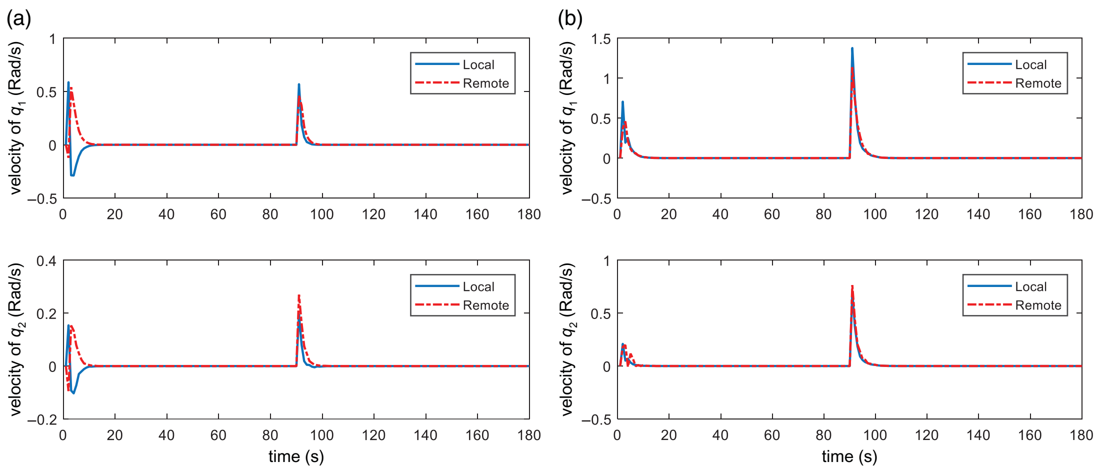

Fig. 6. Velocities in the joint space for teleoperation system in contact with non-passive interaction forces with known passive part, scenario #1, controlled by (a) proposed scheme, (b) method of Islam et al.[22]

https://doi.org/10.1017/S0263574720001277 Published online by Cambridge University Press

Table III. Position errors in joint space.

	MSE (e1) (rad)	MSE (e2) (rad)	Max (e1) (rad)	Max (e2) (rad)
Proposed method	0.076	0.009	2.593	0.845
Method of Islam et al.[22]	18.00	2.299	4.600	1.802

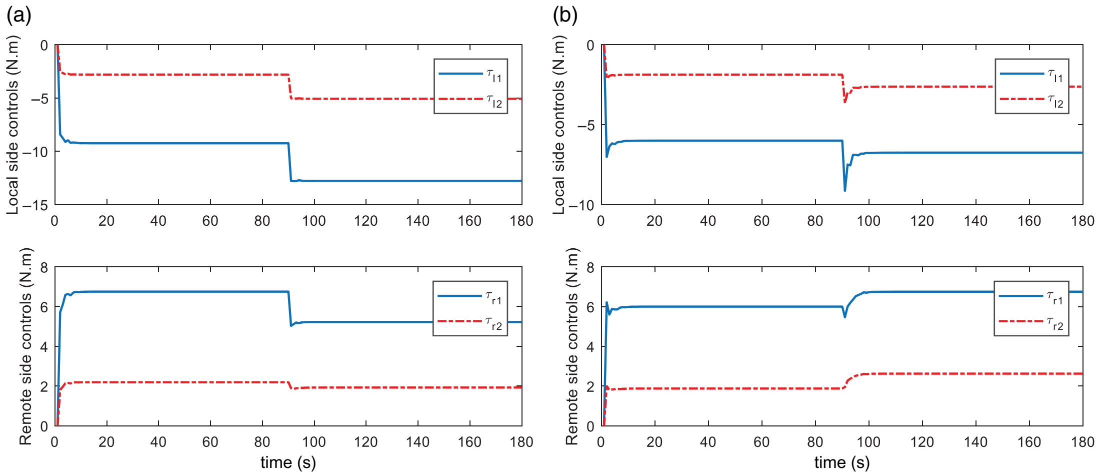

Fig. 7. Control forces of teleoperation system in contact with non-passive interaction forces with known passive part, scenario #1, controlled by (a) proposed scheme, (b) method of Islam et al.[22]

As seen, when the interaction forces are non-passive with passive part in their dynamic, both methods preserve stability of system while the proposed controller can provide better tracking performance than rival one since the position errors converge to zero in our method; because of using the integrals of position errors in IDA-PBC controller (i.e., $f_{24}\int_0^t e_l dt$ and $f_{58}\int_0^t e_r dt$). Note that there are tracking errors in system controlled by other methods.[20–23] Simulation results in scenario #1 confirm this claim. Table III reports the Mean Square Errors (MSEs) and maximum errors for position of links in the joint space, that is $e_k = q_{k_l} - q_{k_r}$. for $k = 1.2$. As seen, the MSEs and maximum errors obtained by our method are considerably lower than the rival ones.

4.1.2. Scenario #2. In the second scenario, the general non-passive interaction forces are considered with no passive parts in their dynamic, that is $S_l = \underline{0}\,.\, D_l = \underline{0}.\;\; S_r = \underline{0}\,.\, D_r = \underline{0}.;\;\; \underline{0} \in \mathbb{R}^{2\times 2}$. So, $\tau_h = \tau_{h0}$ and $\tau_e = \tau_{e0}$, where τ_{h0} and τ_{e0} are bounded signals as depicted in Fig. 4. The simulation results, in this case, are shown in Figs. 8–10.

As seen, for non-passive interaction forces without any known part, the controllers presented in the Islam et al.[22] can't provide stability of system and the positions are increased without limits and velocities are not zero, whereas the proposed controller yields to asymptotic stability of position errors and velocities. Because the position feedback terms in the proposed IDA-PBC (i.e., $f_{21}q_l\,.\, f_{55}q_r$) provide stability when interaction forces are non-passive with no passive part. In other words, if f_{21} and f_{55} in Eqs. (36)–(37) are simultaneously zero, these equations have no solution.

4.2. Experimental verification

In this subsection, real-time implementation results are provided for the platform as shown in Fig. 2. Each manipulator is made of plexi 4mm and is actuated by pair of DC motors MG946, which are capable of producing torque up to 12 Nm with a nominal voltage of 6V and are driven by Arduino Uno. The local and remote manipulators are connected to a laptop via USB ports. The local and remote controllers and communication channel are realized in MATLAB. The time delay in forward and backward paths is shown in Fig. 3.

To sense the angular position and velocity of the links, the platform is equipped with Inertial Measurement Units (IMUs) MPU6050, which include a gyro to measure angular velocities around three axes and an accelerometer to measure linear accelerations in the same axes, as shown in

https://doi.org/10.1017/S0263574720001277 Published online by Cambridge University Press

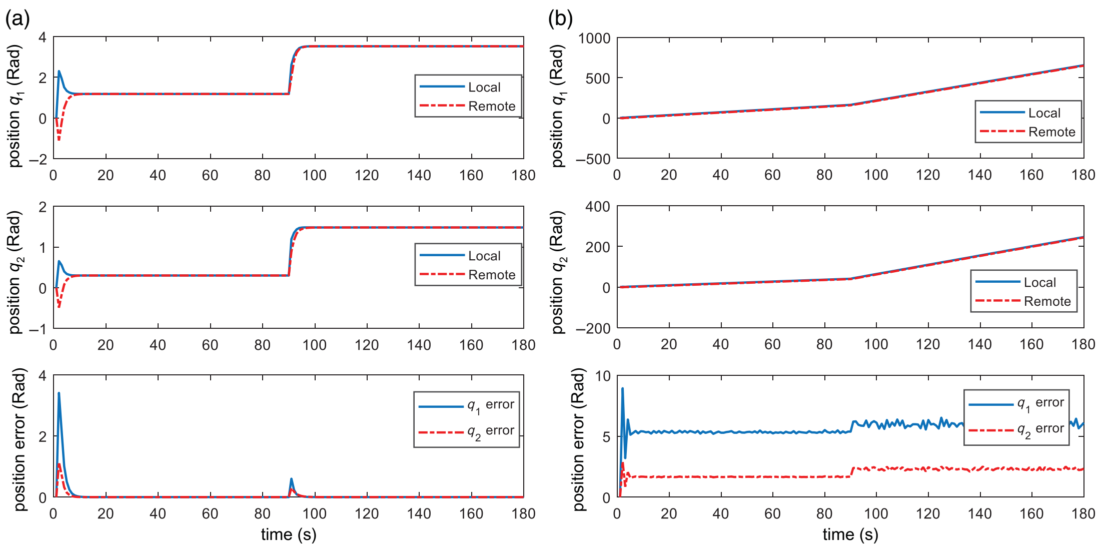

Fig. 8. Positions and positions errors in the joint space for teleoperation system in contact with non-passive interaction forces with no passive part, scenario #2, controlled by (a) proposed scheme, (b) method of Islam et al.[22]

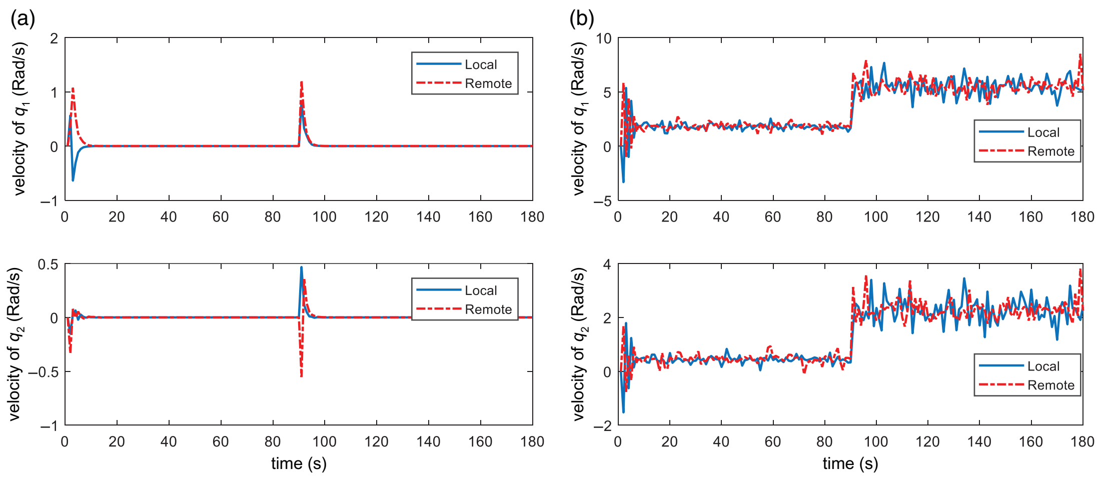

Fig. 9. Velocities in the joint space for teleoperation system in contact with non-passive interaction forces with no passive part, scenario #2, controlled by (a) proposed scheme, (b) method of Islam et al[22]

Fig. 11(a). IMUs are installed on the body of manipulators, as shown in Fig. 11(b). Only the angular velocity around the axis z and the acceleration on the perpendicular axes y and x are directly taken into account, and the angular position is estimated through them. Since the estimation obtained through the acceleration measurements has high-frequency noise, by sensor fusion, the complementary filters are used to estimate the angular position of links by

$$q(kT_s) = (1-\propto)\, q_a(kT_s) + \propto \big(q\,((k-1)\,T_s) + T_s\ \dot{q}(kT_s)\big); \quad q = q_{1_i},\ \ q_{2_i};\ i = l.r, \tag{54}$$

where $q_a = \arctan(\frac{a_y}{a_x})$ is accelerometers angle estimation. The constant $\propto$ is typically close to 1. When it is 1, we obtain the gyro solution, and when it is 0, we obtain the accelerometer solution. Effectively, we will eliminate the drift, while retaining the good short timeframe qualities of the gyro.

The performance of the system is evaluated in both of free motion and in contact with non-passive interaction forces. Consider the case that the human operator act on local manipulator and the remote manipulator has free motion from 0 to 60 s and carry the 80 g weight from time 60 to 140 s. This situation, as shown in Fig. 12, is a non-passive interaction force with no passive part, similar to the scenario #2 in Section 4.1.2. The results of angular position and velocity of manipulator links are

https://doi.org/10.1017/S0263574720001277 Published online by Cambridge University Press

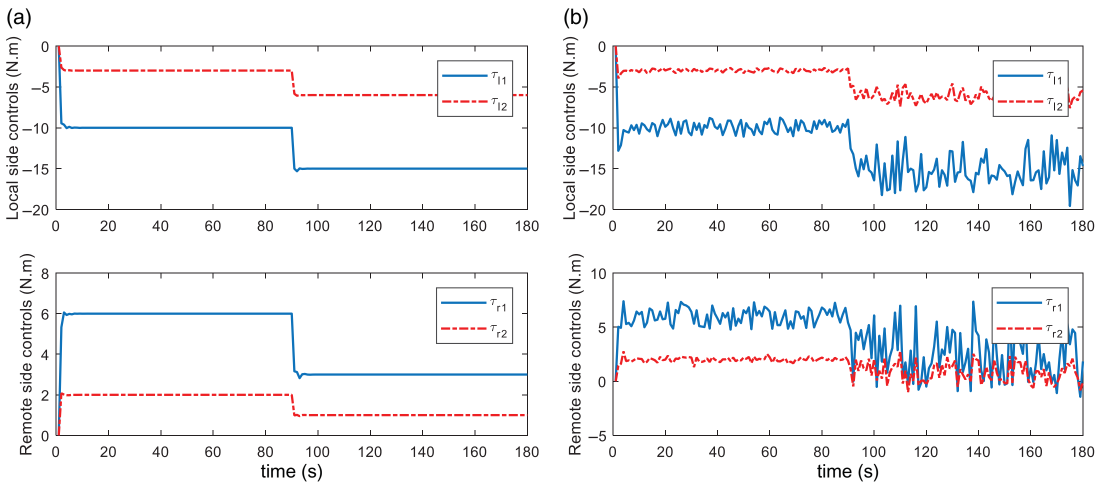

Fig. 10. Control forces of teleoperation system in contact with non-passive interaction forces with no passive part, scenario #2, controlled by (a) proposed scheme, (b) method of Islam et al.[22]

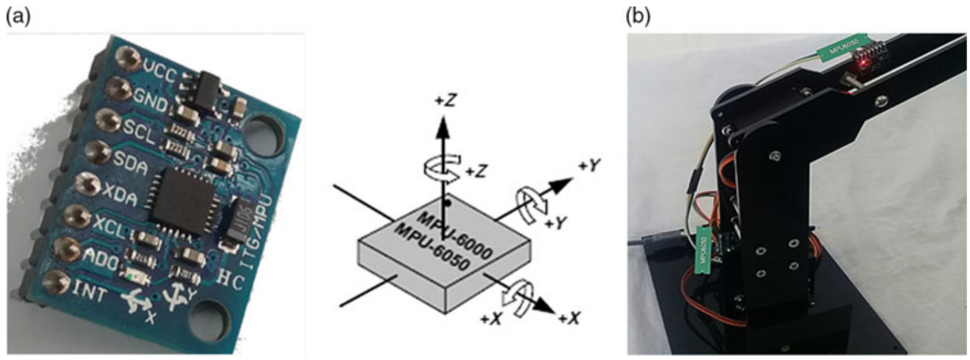

Fig. 11. (a) IMU axes. (b) Installation of IMU on manipulator.

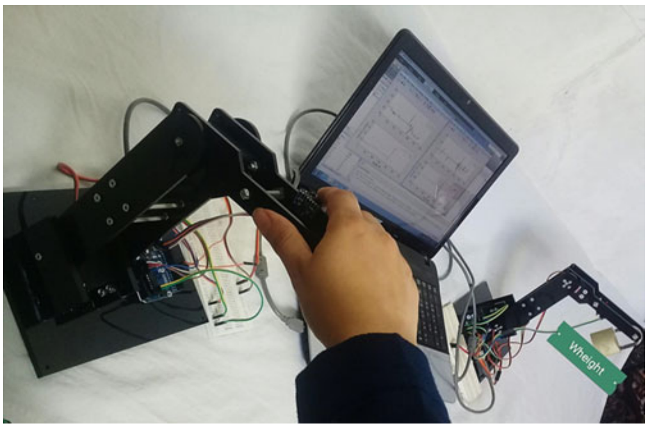

Fig. 12. Laboratory teleoperation system in contact with non-passive environment.

shown in Figs. 13–14(a), which are measured by IMU sensors. Also, the experimental results for the method of Islam et al.[22] are shown in Figs. 13–14(b).

As seen, in free motion from $t = 0$ to 60 s, when the environment force is zero, both methods provide stability and desired performance, but in contact with non-passive interaction forces (carrying the weight) from $t = 60$ to 140 s, only the proposed controller provide asymptotical stability and position tracking and the method of Islam et al.[22] cannot attain stability and tracking objective and

https://doi.org/10.1017/S0263574720001277 Published online by Cambridge University Press

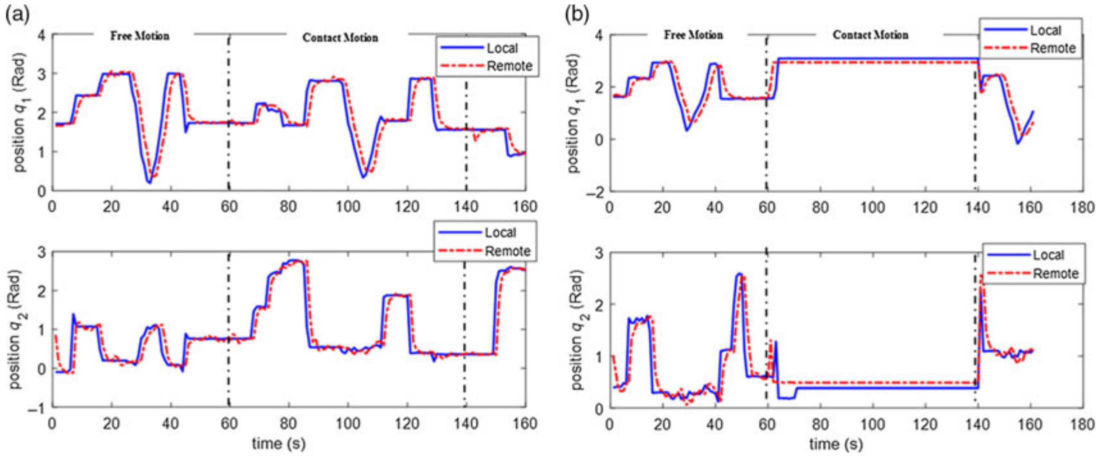

Fig. 13. Angular positions for the teleoperator in contact with non-passive environment, controlled by (a) proposed scheme, (b) method of Islam et al.[22]

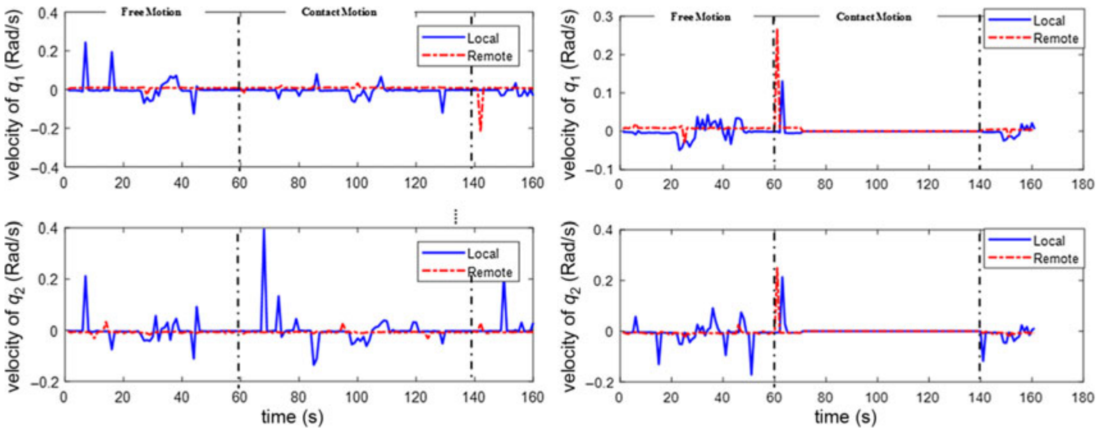

Fig. 14. Angular velocities for the teleoperator in contact with non-passive environment controlled by (a) proposed scheme, (b) method of Islam et al.[22]

the robot links fall due to gravitational forces of weight. Note that in real implementation, the position is limited and cannot be larger than 2π rad.

It is worth noting that in Fig. 14, the peaks of velocities in some times; for instance, $t = 5, 14, 68$ are related to the situations that human operator applies forces to the local manipulator; so, the positions of links are suddenly changed; consequently, great velocities are appeared in the curve. In Fig. 14(b), the peaks of velocities near $t = 60$ correspond to the condition that the external weight is hanged to the remote robot; namely, peripheral force is applied to the remote manipulator. Briefly, peaks in velocity profiles occur when the exogenous forces are exerted on manipulators and consequently the position of links is abruptly altered.

5. Conclusions

This paper has studied the design of bilateral teleoperation system in the presence of asymmetrical time-varying delays in the communication channel, uncertainties in the manipulators' models, and non-passive interaction forces in the terminations. The notion of IDA-PBC has been employed to achieve stable position tracking. The controller parameters are determined by synthesis conditions, which have been obtained via LK theorem to assure robust asymptotic stability of the closed-loop system. The robust asymptotic stability and position tracking in the nonlinear teleoperation system are guaranteed by a new fixed-structure controller whose parameters are computed offline via solving a set of LMIs. The desired performance is achieved without any requirement for known passive parts in the dynamic models of the interaction forces, because of using the position feedback in the controllers. Also, asymptotic stability of the position errors in contact with non-passive interactions is attained because of using the feedback of their integrals in the control law. Comparative simulation and experimental results illustrate the benefits and applicability of the proposed strategy; specifically, mean square errors (MSEs) and maximum errors for the positions of links in the joint space are considerably decreased by the suggested approach compared to a recent rival one. Considering more performance specifications in the design of controller defines future research line.

References

1. P. Hokayem and M. Spong, "Bilateral teleoperation: An historicalsurvey," *Automatica* **42**(12), 2035–2057 (2006).
2. A. Kuzu and E. A. Baran, "Improved bilateral teleoperation with proactive haptic sensing and transmission," *Proc. IMechE Part I: J. Syst. Cont. Eng.* **232**(1), 79–91 (2017).
3. E. Nuno, L. Basanez and R. Ortega, "Passivity-based control for bilateral teleoperation: A tutorial," *Automatica* **47**(3), 485–495 (2011).
4. P. Arcara and C. Melchiorri, "Control schemes for teleoperation with time delay: A comparative study," *Robot. Autom. Syst.* **38**(1), 49–64 (2002).
5. H. C. Hu and Y. C. Liu, "Passivity-based control framework for task-space bilateral teleoperation with parametric uncertainty over unreliable networks," *ISA Trans.* **70**, 187–199 (2017).
6. X. Liu, R. Tao and M. Tavakoli, "Adaptive control of uncertain nonlinear teleoperation systems," *Mechatronics* **24**(1), 66–78 (2014).
7. Y. Yang, C. Hua and X. Guan, "Coordination control for bilateral teleoperation with kinematics and dynamics uncertainties," *Robot. Comput-Integr. Manu.* **30**(2), 180–188 (2014).
8. E. Nuno, R. Ortega, L. Basanez and N. Barabanov, "An adaptive controller for nonlinear bilateral teleoperators," *Automatica* **46**(1), 155–159 (2010a).
9. G. Leung, B. Francis and J. Apkarian, "Bilateral controller for teleoperators with time delay via mu-synthesis," *IEEE Trans. Robot. Autom.* **11**(1), 105–116 (1995).
10. J. Colgate, "Robust impedance shaping telemanipulation," *IEEE Trans. Robot. Autom.* **9**(4), 374–384 (1993).
11. S. Sirouspour, "Modeling and control of cooperative teleoperation systems," *IEEE Trans. Robot.* **21**(6) 1220–1225 (2005).
12. L. Mohammadi, A. Alfi and B. Xu, "Robust bilateral control for state convergence in uncertain teleoperation systems with time-varying delay: Aguaranteed cost control design," *Nonlinear Dyn.* **88**(2), 1413–1426 (2017).
13. A. Shahdi and Sh. Sirouspour, "Adaptive/robust control for time-delay teleoperation," *IEEE Trans. Robot.* **25**(1), 196–205 (2009).
14. I. Sharifi, H. A. Talebi and M. Motaharifar, "Robust output feedback controller design for time-delayed teleoperation: Experimental results," *Asian J. Cont.* **19**(2), 1–11 (2017).
15. D. Sun, Q. Liao and H. Ren, "Type-2 fuzzy modeling and control for bilateral teleoperation system with dynamic uncertainties and time-varying delays," *IEEE Trans. Ind. Elec.* **65**(1), 447–459 (2017).
16. T. Q. Dinh et al., "Sensorless force feedback joystick control for teleoperation of construction equipment," *Int. J. Precision Eng. Manu.* **8**(7), 955–996 (2017).
17. M. Dyck, A. Jazayeri and M. Tavakoli, "Is the Human Operator in a Teleoperation System Passive?" *Proceeding of the IEEE world Haptics Conference* (2013) pp. 683–688.
18. F. Hashemzadeh and M. Tavakoli, "Position and force tracking in nonlinear teleoperation system under varying delays," *Robotica* **33**(4), 1003–1016 (2015).
19. S. Ganjefar, S. Rezaei and F. Hashemzadeh, "Position and force tracking in nonlinear teleoperation systems with sandwich linearity in actuators and time-varying delay," *Mech. Syst. Signal Process.* **86**(part A), 308–324 (2017).
20. C. Hua and P. X. Liu, "Convergence analysis of teleoperation systems with unsymmetric time-varying delays," *IEEE Trans. Circ. Syst. II* **56**(3), 240–244 (2009).
21. A. Jazayeri and M. Tavakoli, "Bilateral teleoperation system stability with non-passive and strictly passive operator or environment," *Cont. Eng. Pract.* **40**, 45–60 (2015).
22. SH. Islam, P. X. Liu and A. El Saddik, "Nonlinear control for teleoperation systems with time varying delay," *Nonlinear Dyn.* **76**, 931–954 (2014).
23. SH. Islam, P. X. Liu, A. E. L. Saddik and J. Dias, "Bilateral shared autonomous systems with passive and non-passive input forces under time varying delay," *ISA Trans.* **54**, 218–228 (2015).
24. R. Ortega and E. Garcia-Canseco, "Interconnection and damping assignment passivity-based control: A survey," *Eur. J. Cont.* **10**(5), 432–450 (2004).
25. T. Hatanaka, N. Chopra, M. Fujita and M. W. Spong, *Passivity-Based Control and Estimationin Networked Robotics* (Springer International, Switzerland, 2015).
26. M. Erlic and W. S. Lu, "Manipulator Control with an Exponentially Stable Velocity Observer," *Proceeding of the IEEE American Control Conference* (1992) pp. 1241–1242.